The Third International Bridge Seismic Workshop, 3rd IBSW
Seattle, Washington, USA - October 1st to 4th, 2019

3-D GROUND-MOTION SIMULATIONS OF MAGNITUDE 9 EARTHQUAKES ON THE CASCADIA SUBDUCTION ZONE

A. Frankel[1], E. Wirth[2], N. Marafi[3], J. Vidale[4], and W. Stephenson[5]

[1] *Research Geophysicist, U.S. Geological Survey, afrankel@usgs.gov*
[2] *Research Geophysicist, U.S. Geological Survey, ewirth@usgs.gov*
[3] *Postdoctoral Associate, University of Washington, marafi@uw.edu*
[4] *Professor, University of Southern California, seismoguy@mac.com*
[5] *Research Geophysicist, U.S. Geological Survey, wstephens@usgs.gov*

Abstract

We have produced a large set of broadband (0-10 Hz) synthetic seismograms for moment magnitude 9 earthquakes on the Cascadia subduction zone using 3D finite-difference simulations and stochastic synthetics, as part of the M9 Project. These simulated ground motions are being used to assess building and bridge performance and to predict liquefaction and landslides. The 3D velocity model is based on extensive seismological and geological studies. 3D finite-difference synthetics were calculated up to 1 Hz and combined with higher-frequency (1-10 Hz) stochastic synthetics using matched filters. Our earthquake source model consists of deep, high stress drop, magnitude 8 sub-events superimposed on shallower background slip with long rise times and lower stress drop, based on observations of the M_w 9.0 Tohoku, Japan and M_w 8.8 Maule, Chile earthquakes. A total of 50 3D simulations were run using a range of rupture parameters. The synthetic ground motions exhibit long durations of shaking and large variations in response spectra caused by rupture directivity and the proximity to the nearest sub-event. For sites outside of the sedimentary basins, we find that the response spectra of the synthetics bracket the values from the BC Hydro ground motion prediction equations (GMPE) at periods from 0.1-6 s, but exceed these GMPEs at periods greater than 6 s. We determined amplification factors of 2-5 at periods of 1-10 s in the Seattle basin, compared to sites outside the basin. This amplification is larger than the basin factors found from crustal earthquakes in the NGA West 2 GMPEs.

1. Introduction

The estimated probability of a moment magnitude M_w 9 earthquake on the Cascadia subduction zone is 10-14% in the next 50 years, based on paleoseismic evidence and the occurrence of the previous earthquake in 1700 [1]. Therefore, it is critical to estimate the range of expected ground motions from such earthquakes and their effects on the built environment. In this paper, we describe the results from 3D simulations for 30 rupture scenarios of M_w 9 Cascadia earthquakes. These simulations produce a range of expected ground motions over a frequency band from co-seismic offset to 10 Hz. We also conducted 20 simulations to determine the sensitivity of the synthetic seismograms and response spectra to various rupture parameters. This study was part of the M9 Project at the University of Washington that was funded by the National Science Foundation. The U.S. Geological Survey was a collaborator in this effort. We have posted approximately 2.5 million broadband synthetic seismograms on the DesignSafe website: https://www.designsafe-ci.org/data/browser/public/designsafe.storage.published/PRJ-1355, along with response spectra. Complete descriptions of the methodology, results, and sensitivity studies of the 3D simulations are given in [2] and [3].

2. Methodology

The simulations were conducted using a 3D finite-difference program that has variable grid spacing with depth [4]. The 3D velocity model was based on a large set of seismological, geophysical, and geological data [5]. The simulations were run on supercomputers with 500 to 1000 processing cores. The minimum shear-wave velocity was 600 m/s. The 3D simulations are accurate up to 1 Hz. For higher frequencies, we summed stochastic seismograms with delays based on rupture propagation. The synthetics from the 3D simulations and the stochastic procedure were combined using matched filters to produce broadband synthetics from 0-10 Hz.

We are especially interested in the seismic response of deep sedimentary basins, such as the Seattle and Tacoma basins. Observations have shown that these basins amplify and prolong ground shaking at periods of about 1 s and longer. The portion of the 3D velocity model for the Seattle basin was validated by modeling the M_w 6.8 Nisqually earthquake and a M4.8 earthquake, as well as the basin amplification from four local earthquakes [6].

The M9 earthquake rupture model was informed by observations from the M_w 8.8 Maule, Chile and M_w 9.0 Tohoku, Japan earthquakes [7, 8]. This compound rupture model consists of high stress drop sub-events located in the deeper portion of the rupture zone and larger background slip in the shallow portion of the rupture zone (Fig. 1). The sub-event slip is superimposed on the background slip. The shallow background slip accumulates too slowly to produce substantial strong ground motions with periods less than about 7 s. The shallow portion of the background slip is the key cause of the tsunami. We used M_w 8 sub-events in the simulations, similar to the magnitudes of the sub-events observed in the Maule and Tohoku earthquakes. We distributed five sub-events along the length of the rupture zone, so that the average spacing between sub-events was similar to that observed in the Tohoku earthquake. These sub-events radiate most of the strong ground motions in the periods of engineering interest (< 10 s).

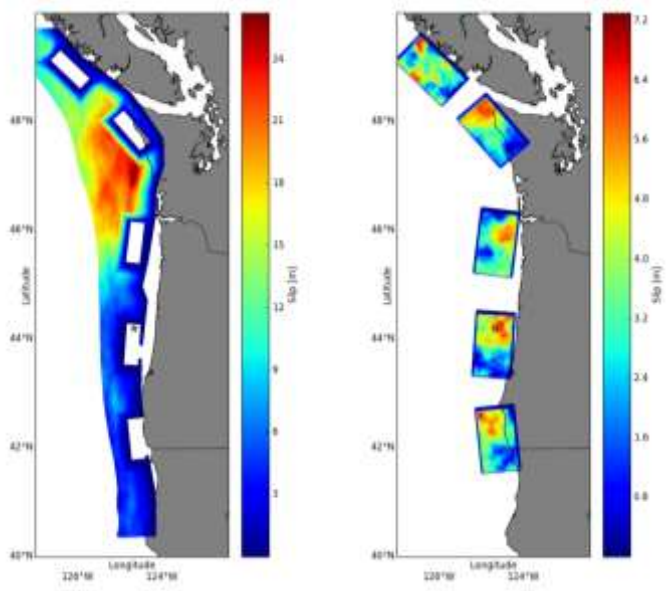

Fig. 1. Compound slip model for run 21. Background slip is shown on the left and tapers to zero in the sub-event locations. M_w 8.0 sub-events are shown on the right. The sub-event slip is superimposed on the background slip. The small star is the hypocenter.

2. Results

Fig. 2 shows maps of response spectral accelerations (SA) for 0.2 and 3.0 s derived from one of the 30 simulations (run 21). For 0.2 s SA, the results are dominated by the stochastic procedure, which used a site condition with a Vs30 of 600 m/s. The 3.0 s SA values are controlled by the 3D simulations. In both period bands, the ground motions are highest near the locations of the sub-events. The map of 3.0 s SA exhibits strong amplification by the Seattle and Tacoma basins within the Puget Lowland. Rupture directivity effects are also apparent in the 3.0 s SA map, with higher ground motions extending inland from the sub-events.

Synthetic acceleration seismograms exhibit relatively long durations of strong shaking (Fig. 3). For this run, sites at Newport and Seaside, OR near the coast have peak ground accelerations (PGA) of about 0.6 g. Sites in Seattle and Portland, more distant from the rupture, have PGAs of 0.1-0.2g. There is strong variation in PGA for sites along the coast, controlled by the proximity to the sub-events. This is seen by the factor of 2 variation in PGA between SEAW (Seaside) and sites S2 and S3 which are 50 and 100 km, respectively, to the south (Fig. 3).

Large amplifications of long-period (1-10 s) SA values are found for the Seattle and Tacoma basins in the Puget Lowland (Fig. 4). In general, the amplifications are higher for sites with larger values of Z2.5, which is the depth to a shear-wave velocity of 2.5 km/s. The velocity synthetics in Fig. 4 illustrate the large amplification for the site in the Seattle basin (QAW), compared to a site just south of the basin (SP2) and one west of the Puget Lowland (DOSE).

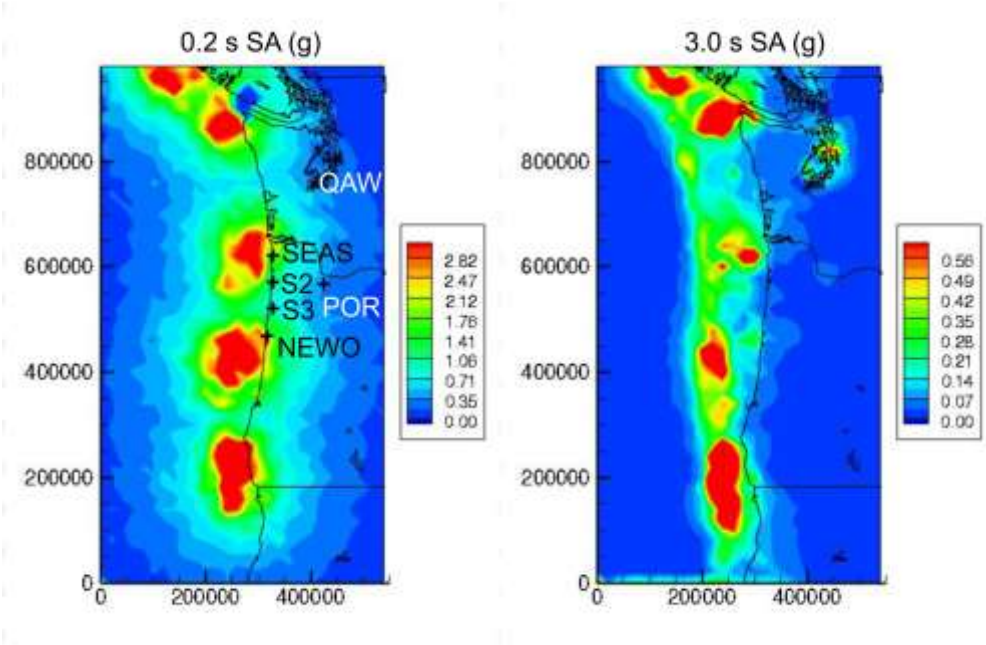

Fig. 2. Maps of SA values (in *g*) from the synthetics for run 21

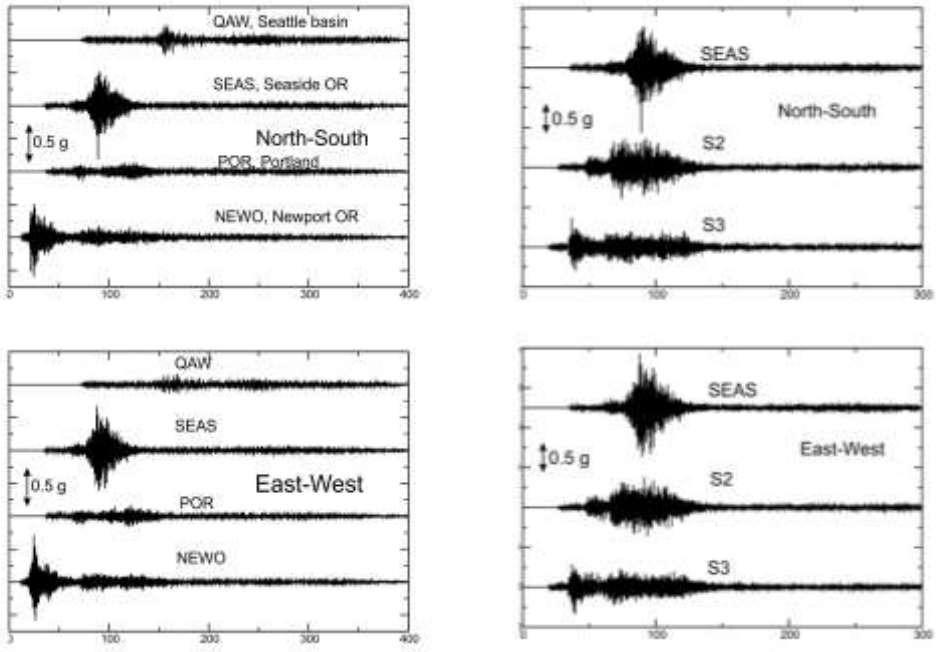

Fig. 3. Synthetic acceleration seismograms for run 21. Site locations are shown in Fig. 2.

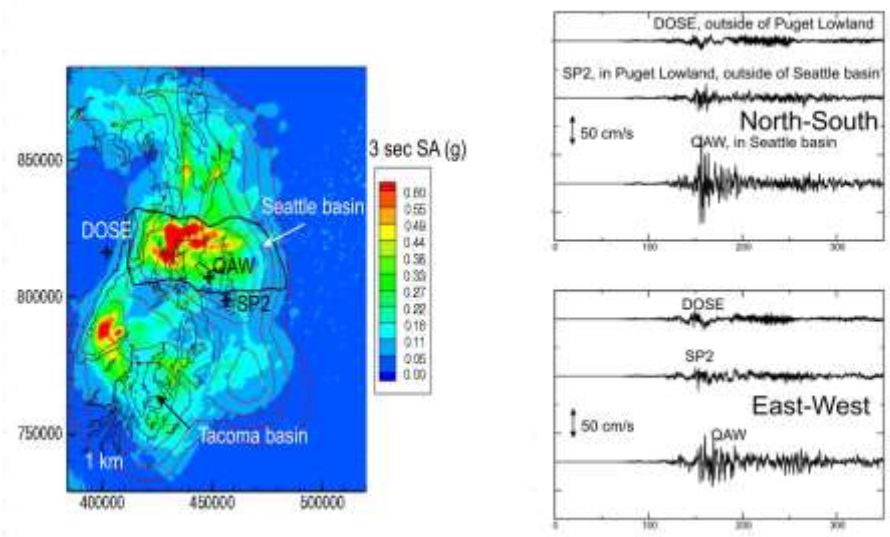

Fig. 4. (left) Map of 3 s SA in the Puget Lowland for run 21. The contours depict the Z2.5 values (depth to shear wave velocity of 2.5 km/s), with 1 km contour interval. Outline of Seattle basin from R. Blakely (written comm., 2017). (right) Synthetic velocity seismograms for a site in the Seattle basin and two sites outside the basin (see map on left for locations).

In total, we ran 30 3D simulations, varying the starting point (hypocenter) of rupture, the slip distributions of the sub-events and background slip, and the locations of the sub-events. Fig. 5 shows the hypocenters and sub-event locations for the 30 runs. The location of the down-dip (eastern) edge of the rupture zone was also varied, using locations and weights from the 2014 National Seismic Hazard Maps.

In Fig. 6 we compare the SA values from the synthetics at non-basin sites to the predictions of the BC Hydro ground motion prediction equations (GMPE) [9] for a Vs30 of 600 m/s. This GMM was based on strong-motion data for interface subduction zone earthquakes. For periods up to 6 s, the median values of the synthetics are similar to those of the BC Hydro GMPE (Fig. 6). However, for 7.5 s SA, the synthetics have higher values and a more gradual fall-off with distance than the BC Hydro predictions. This may be due to the shallower depth of the M9 sub-events compared to those in the Maule and Tohoku earthquakes. Note that the observed 3 s SA values at close-in stations from the M_w 8.8 Maule earthquake are similar to the simulations. For 0.2 and 1.0 s, some of the Maule data are higher than the M9 simulations, but many of these sites with Maule earthquake recordings have Vs30 values less than the 600 m/s used in the simulations.

The M9 simulations display strong amplification of 1-10 s SA in the Seattle and Tacoma sedimentary basins. Fig. 7 shows the basin amplification factors (BAF) found for the Seattle basin. We determined the basin amplification at sites in the Seattle basin with Z2.5 greater than 5 km, referenced to sites outside the Puget Lowland with Z2.5 equal to 1 km (Fig. 7). We found amplification factors of 4-5 at periods of 2 to 6 s. When referenced to a site just to the south the Seattle basin, we determined amplification factors of 2-3. We found similar amplification factors from recordings of a M5.0 earthquake located just below the plate interface near the potential down-dip rupture edge of a M9 earthquake [2]. These amplification factors are much higher than those determined for crustal earthquakes from an NGA West 2 GMPE [10], for sites with similar Z2.5 values as the Seattle basin [2]. The larger amplification for the M9 earthquakes is likely caused by the more horizontal propagation of S-waves from Cascadia M9 earthquakes compared to those of crustal earthquakes near or underneath a basin. This will lead to larger basin-edge generated surface waves. Furthermore, the shallow M9 source produces substantial long-period surface waves that are strongly amplified by the Seattle basin [2].

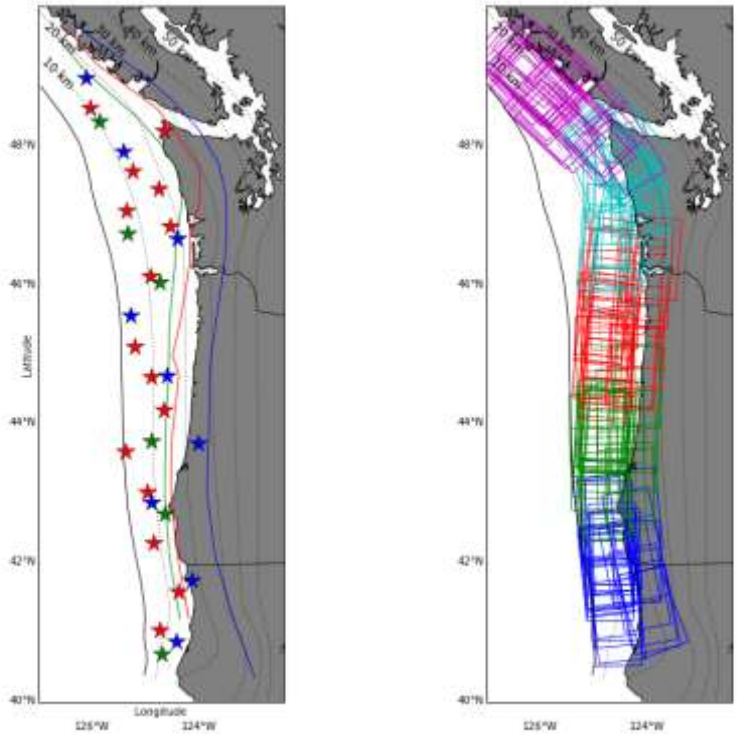

Fig. 5. (left) distribution of hypocenters (stars) used in the 30 runs. Colored lines denote three choices for down-dip (eastern) edge of rupture. Hypocenters are color coded to correspond to the down-dip edge used for that run. (right). Locations of sub-events used in the 30 runs.

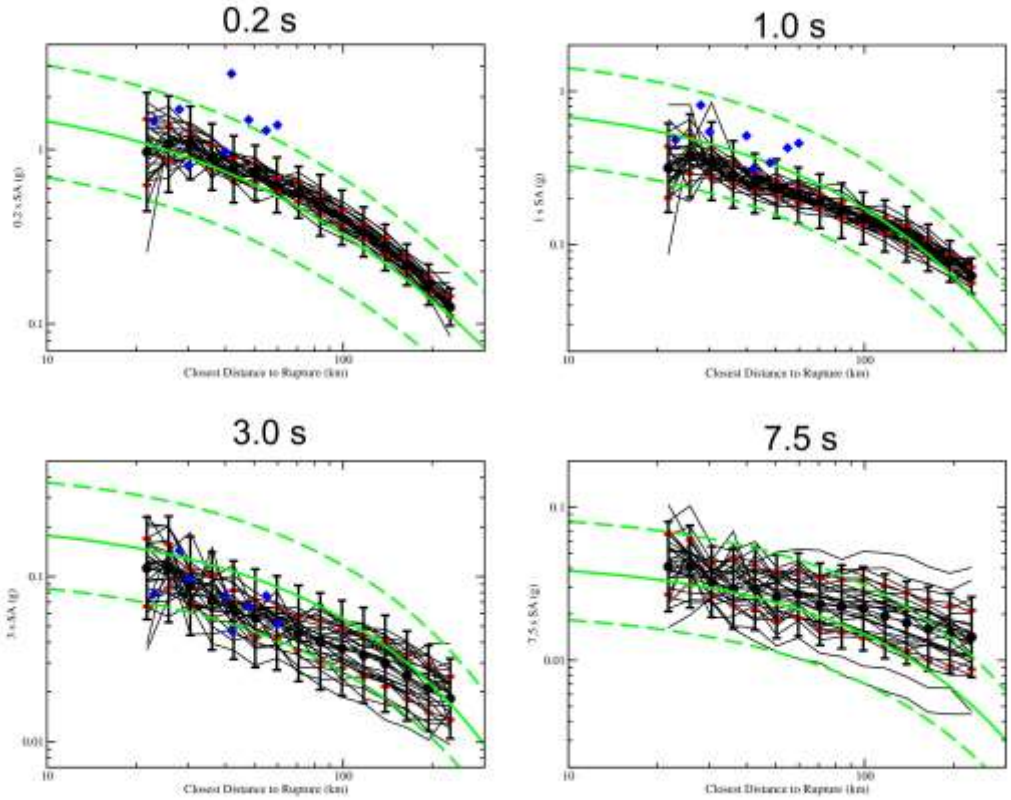

Fig. 6. Results of 30 runs for non-basin sites. Each black line is the log-averaged SA for one of the 30 runs. Black dots are the log-averaged values for all 30 runs. Black error bars correspond to total standard deviation in that distance bin. Red error bars denote inter-event standard deviations. Green lines are predictions for M_w 9.0 from the BC Hydro GMPE [9], with ± one standard deviation. Blue diamonds are SA values from close-in recordings of the M_w 8.8 Maule earthquake.

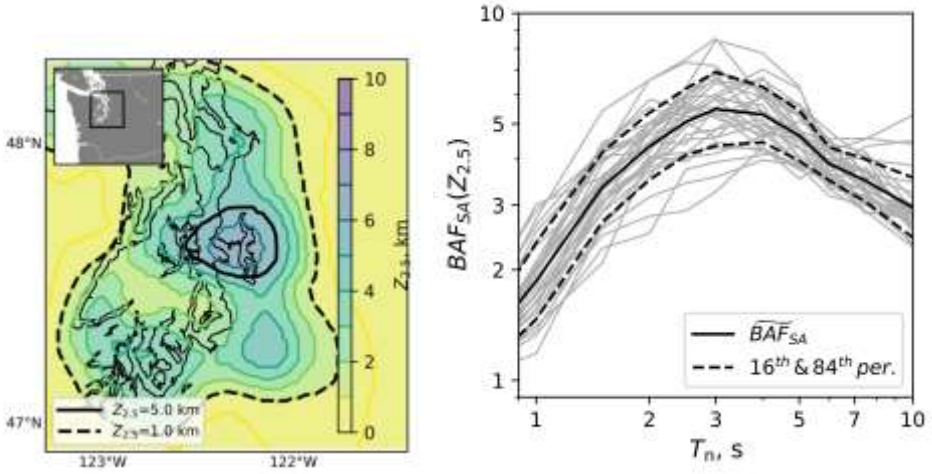

Fig. 7. (left) Map showing Z2.5 for Puget Lowland. (right) Basin amplification factors (BAF) calculated for sites with Z2.5 >= 5.0 km, referenced to sites with Z2.5= 1.0 km, based on the 30 3D simulations.

3. Conclusions

The 30 sets of M_w 9 broadband synthetics, using a range of hypocenters, sub-event locations, slip distributions, and down-dip edge geometries, provide a useful range of expected ground motions. We find larger variability of SA for sites closer to the rupture, due to the proximity to the sub-events and rupture directivity. For periods of 0.1 to 6 s the SA values at non-basin sites from the synthetics are similar to those from the BC Hydro GMPE. Large amplification factors are found in the Seattle basin in the M_w 9 synthetics at 1 – 10 s period, relative to sites south of the basin and sites outside the Puget Lowland. These basin amplification factors are larger than those reported in GMPE for crustal earthquakes. The synthetic seismograms produced in this work are being used to evaluate vulnerability of structures and ground failure from the expected shaking from a M_w 9 Cascadia earthquake. These results will help to improve hazard and risk assessments in the Cascadia region and increase public safety.

4. Acknowledgements

We thank Pengcheng Liu of the U.S. Bureau of Reclamation for providing the finite-difference simulaiton program. This work was partly supported by National Science Foundation grant EAR-1331412. The authors acknowledge the Texas Advanced Computing Center at the University of Texas at Austin, Pacific Northwest National Laboratory, and the University of Washington for providing high performance computing resources that contributed to the results reported in this paper.

5. References

[1] Petersen, M.D., Cramer, C.H., and Frankel, A.D., (2002): Simulations of seismic hazard for the Pacific Northwest of the United States from earthquakes associated with the Cascadia subduction zone, *Pure and Applied Geophysics*, **159**, 2147-2168.

[2] Frankel, A.D., Wirth, E.A., Marafi, N., Vidale, J.E., and Stephenson W.J. (2018): Broadband synthetic seismograms for magnitude 9 earthquakes on the Cascadia megathrust based on 3D simulations and stochastic synthetics (Part 1): Methodology and Overall Results, *Bulletin of Seismological Society of America*, doi: 10.1785/0120180034.

[3] Wirth, E.A., Frankel, A.D., Marafi, N., Vidale, J.E., and Stephenson, W.J. (2018): Broadband synthetic seismograms for magnitude 9 earthquakes on the Cascadia megathrust based on 3D simulations and stochastic synthetics (Part 2): Rupture parameters and variability, *Bulletin of Seismological Society of America*, doi: 10.1785/0120180029.

[4] Liu, P.C. and Archuleta, R.J. (2002): The effect of a low-velocity surface layer on simulated ground motion, *Seismological Research Letters*, **37**, L13301.

[5] Stephenson, W.J., Reitmann, N.G., and Angster, S.J. (2017): P- and S-wave velocity models incorporating the Cascadia subduction zone for 3D earthquake ground motion simulations, Update for OFR 2007-1348: *U.S. Geological Survey Open-File Report 2017–1152*, 17pp, https://doi.org/10.3133/ofr20171152.

[6] Frankel, A., Stephenson, W. and Carver, D. (2009): Sedimentary basin effects in Seattle, Washington: ground-motion observations and 3D simulations, *Bulletin of the Seismological Society of America* 2009; **99**, 1579-1611.

[7] Frankel A. (2013): Rupture history of the 2011 M9 Tohoku Japan earthquake determined from strong-motion and high-rate GPS recordings: sub-events radiating energy in different frequency bands. *Bulletin of the Seismological Society of America*, **103** (2B): 1290-1306.

[8] Frankel A. (2017): Modeling strong-motion recordings of the 2010 M_W 8.8 Maule, Chile earthquake with high stress-drop subevents and background slip. *Bulletin of the Seismological Society of America*, **107** (1): 372-386.

[9] Abrahamson, N, Gregor, N., and Addo, K. (2016): BC Hydro ground motion prediction equations for subduction earthquakes, *Earthquake Spectra*, **32** (1): 23-44.

[10] Campbell, K.W. and Borzorgnia, Y. (2014): Ground motion model for the average horizontal components of PGA, PGV, and 5% damped linear acceleration response spectra, *Earthquake Spectra*, **30**, 1087-115.